

Supporting Information for: Segmentation of the Main Himalayan Thrust illuminated by Bayesian inference of interseismic coupling

Luca Dal Zilio^{1,2*}, Romain Jolivet³, Ylona van Dinther^{1,4}

¹ Department of Earth Sciences, ETH Zürich, Sonneggstrasse 5, 8092 Zürich, Switzerland

² Seismological Laboratory, California Institute of Technology, Pasadena, California

³ Département de Géosciences, Ecole Normale Supérieure, Paris, France

⁴ Department of Earth Sciences, Utrecht University, The Netherlands

Contents of this file

1. Tables S1 and S2
2. Figures S1 to S7
3. Supporting References

Longitude	Slip rate (mm/yr)	Uncertainty (mm/yr)	Azimuth ($^{\circ}$ E)	Reference
78.0	13.1	0.8	18	Thakur et al. (2014)
82.0	19.0	1.5	12	Mugnier et al. (2004)
85.8	18.2	6.0	8	Bollinger et al. (2014)
90.3	20.8	8.8	-5	Berthet et al. (2014)

Table S1. Long term slip rates and uncertainties from geomorphic studies used in this study.

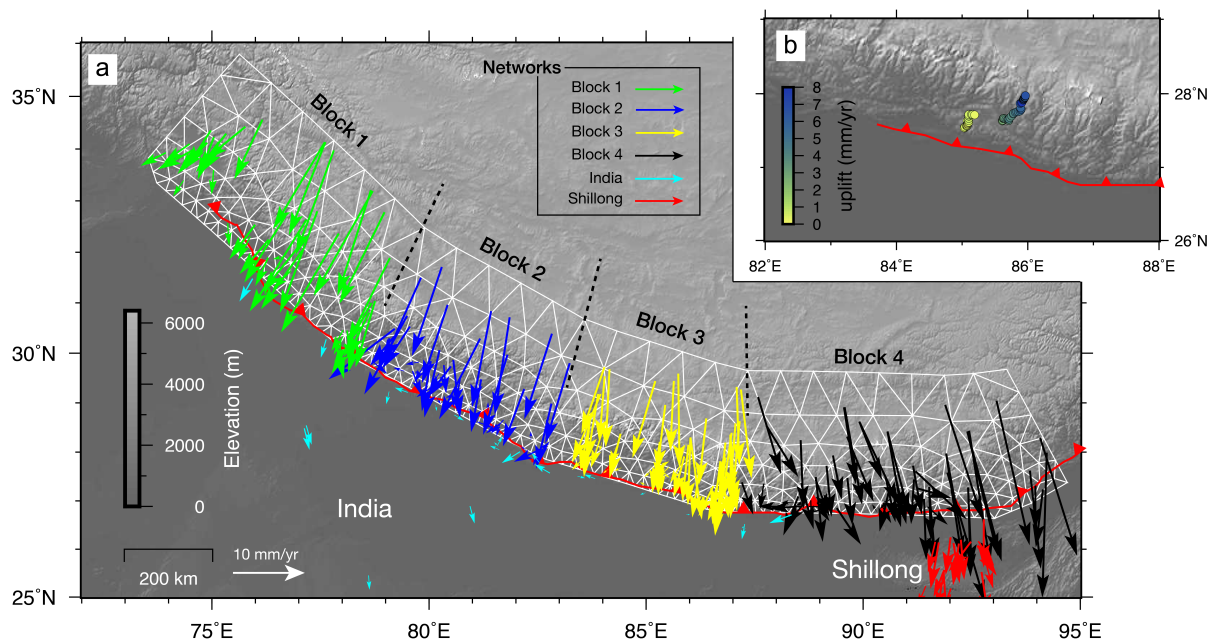


Figure S1. Top view of the fault and GPS network (in the fixed-Indian reference frame) and levelling measurements employed in this study. **a**, GPS network is divided in the following subnetworks: block-1 (green), block-2 (blue), block-3 (yellow), block-4 (black), India (light blue), and Shillong (red). Dashed black lines are the boundaries between different regions of uniform long term slip rate. White triangular mesh is the fault discretization used in this model. **b**, Levelling data. The red line shows the surface trace of the Main Frontal Thrust.

Event	Year	Mw	Reference
Lo Mustang	1505	8.2	Bilham (2004); Ambraseys and Douglas (2004); Bilham and Ambraseys (2005); Bollinger et al. (2016)
Kashmir	1555	7.6	Bilham (2004); Ambraseys and Douglas (2004)
Bhutan	1714	8.1	Hetényi et al. (2016); Le Roux-Mallouf et al. (2016)
Uttar-Pradesh	1803	7.5	Ambraseys and Jackson (2003); Bilham (2004)
Kangra	1905	7.8	Wallace et al. (2005); Hough and Bilham (2008); Ambraseys and Douglas (2004)
Bihar-Nepal	1934	8.2	S. Sapkota et al. (2013); S. N. Sapkota et al. (2016); Hough and Bilham (2008)
Assam	1950	8.7	Khatttri (1987); Bilham (2004)
Kashmir	2005	7.6	Bendick et al. (2007); Pathier et al. (2006); Avouac et al. (2006)
Gorkha	2015	7.8	Avouac et al. (2015); Duputel et al. (2016); Galetzka et al. (2015); Lindsey et al. (2015)

Table S2. List of the major historical earthquakes across the Himalayan arc.

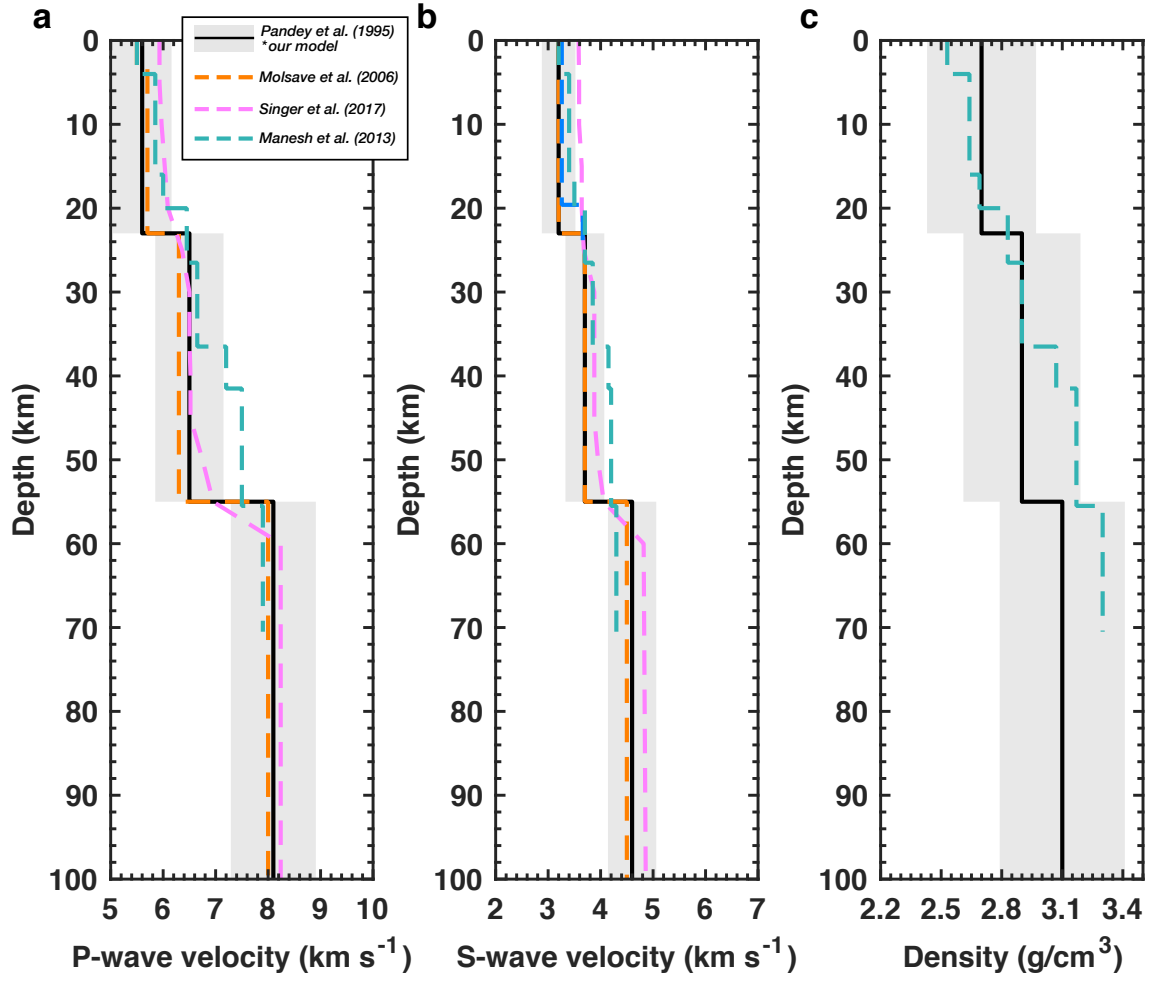


Figure S2. Earth model: (a) P-wave velocity, (b) S-wave velocity and (c) Density used in this study for Green's function (GF) calculations. The layered model used in this study for Green's function (GF) calculations is plotted as a solid black line (Pandey et al., 1995). Dashed lines refer to the other models used to constrain the uncertainties on model prediction (Mahesh et al., 2013; Monsalve et al., 2006; Singer et al., 2017). Grey areas are the standard deviation of the probability density function, representing our confidence level on the elastic properties, as used to build the model prediction error (C_p).

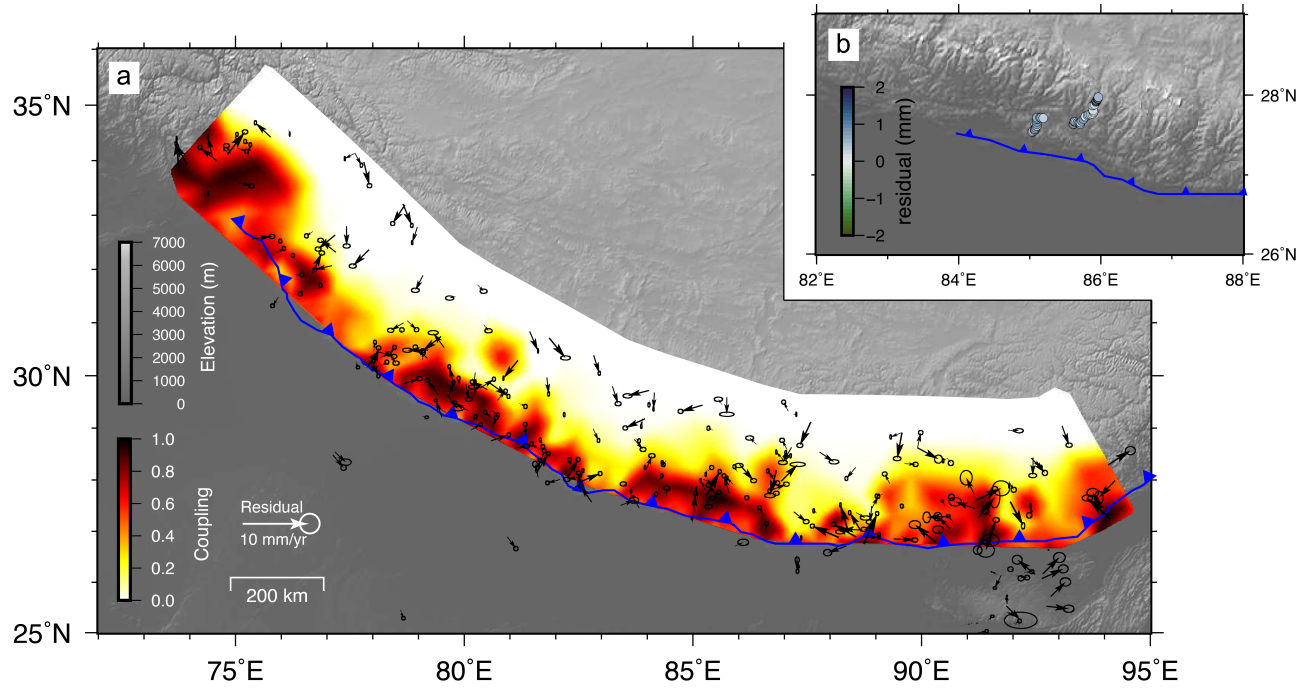


Figure S3. Posterior mean coupling model of the Himalayan megathrust shown in Fig. 2 and residuals of (a) GPS data (with uncertainty ellipses) and (b) levelling data. Ellipses show the uncertainties at the 67% confidence level.

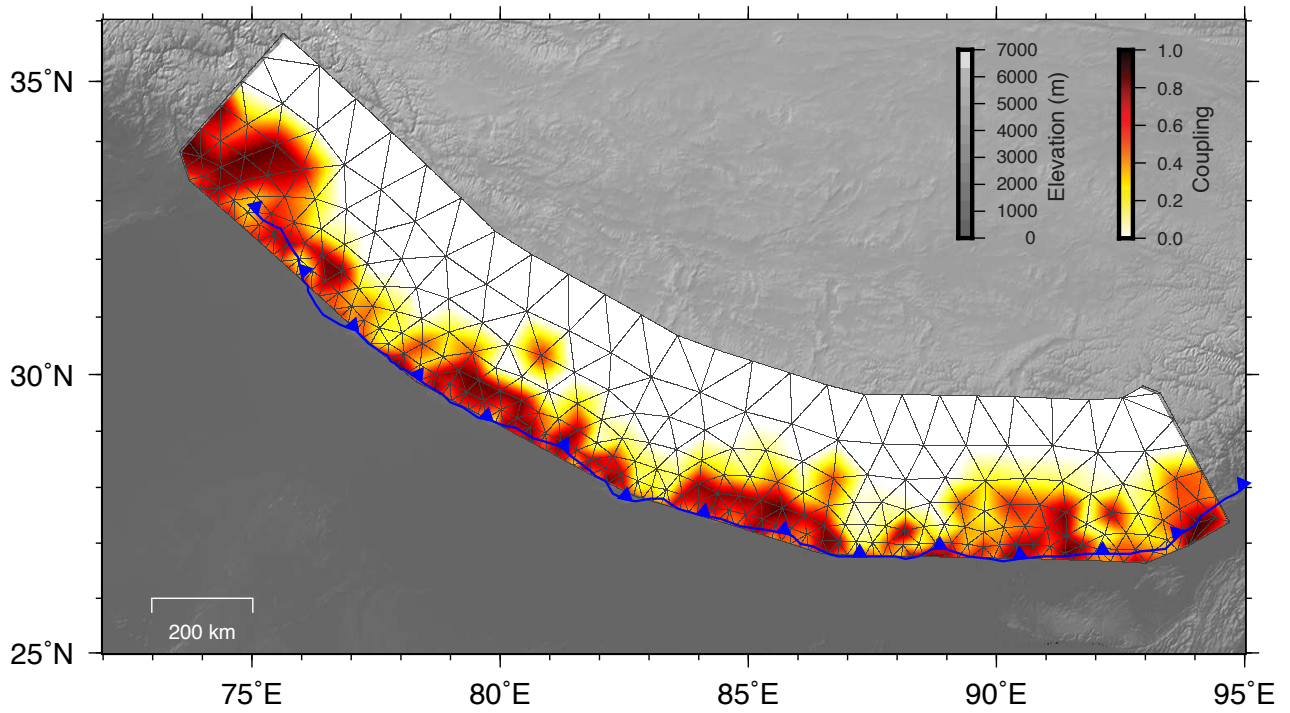


Figure S4. Posterior mean coupling model assuming a homogeneous convergence rate. The resulting posterior mean coupling model is obtained assuming a constant convergence rate along-strike, with no along-strike blocks (see Fig. S1). Thin black lines represent the fault parametrization. Solid blue line shows the surface trace of the Main Frontal Thrust.

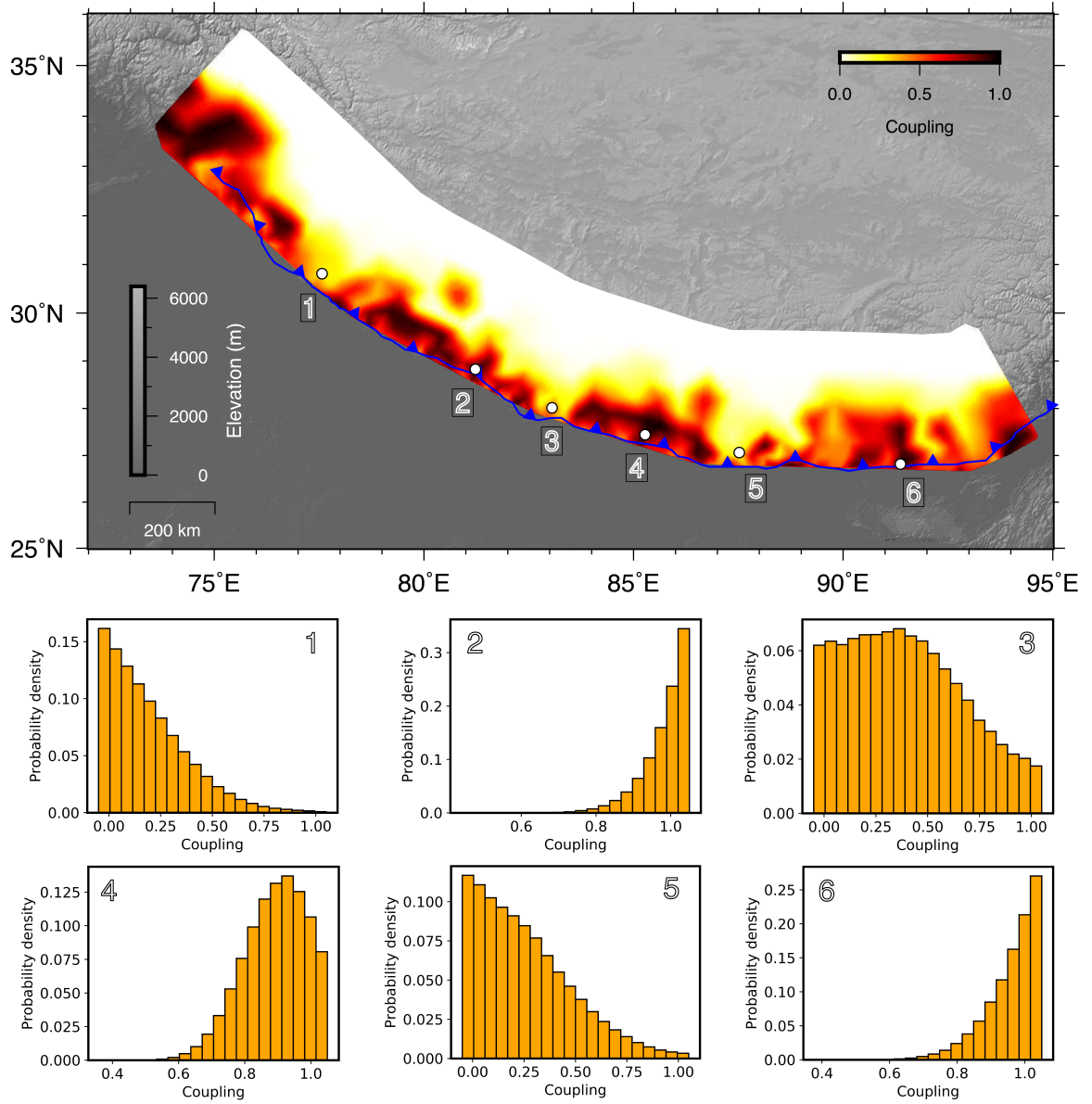


Figure S5. Posterior mean coupling model assuming 5% uncertainty on the elastic properties of each layer of the elastic half-space (see Methods for details). For each of the histograms, orange bars are the marginal probability densities at discrete nodes of the fault model. Solid blue line shows the surface trace of the Main Frontal Thrust.

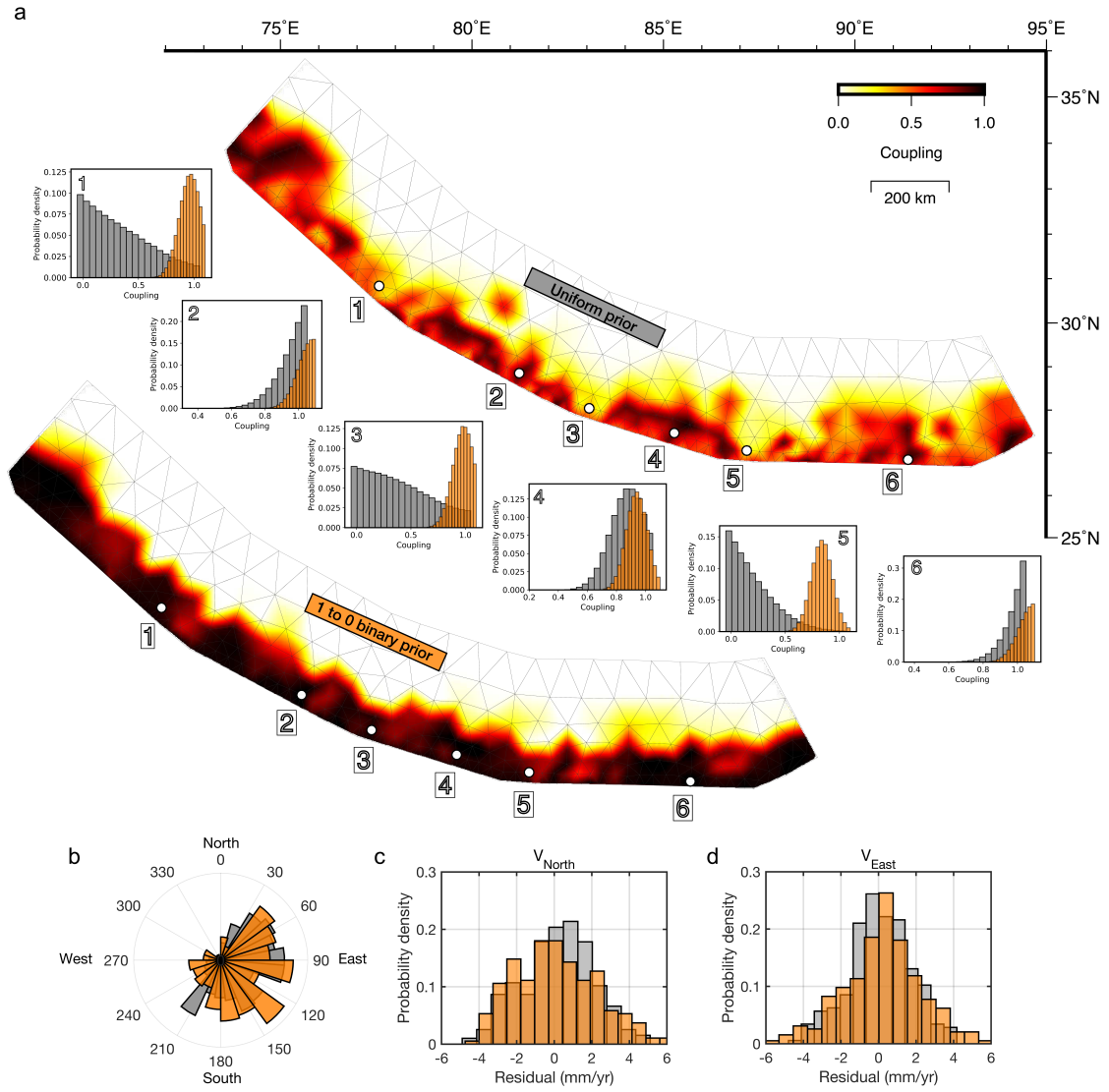


Figure S6. Comparison of coupling models, probability density functions and residuals of the GPS data. **a**, Top: posterior mean solution shown in Fig. 2 assuming a uniform prior. Bottom: posterior mean solution of model incorporating a strongly constrained 0-to-1 binary prior. Histograms indicate the marginal probability densities at discrete 6 nodes of the fault of models with uniform prior (grey) and binary prior (orange). **b**, Rosetta histograms showing the orientation of the residuals of the two models. **c–d**, Probability density distributions of residuals on both north and east velocity components.

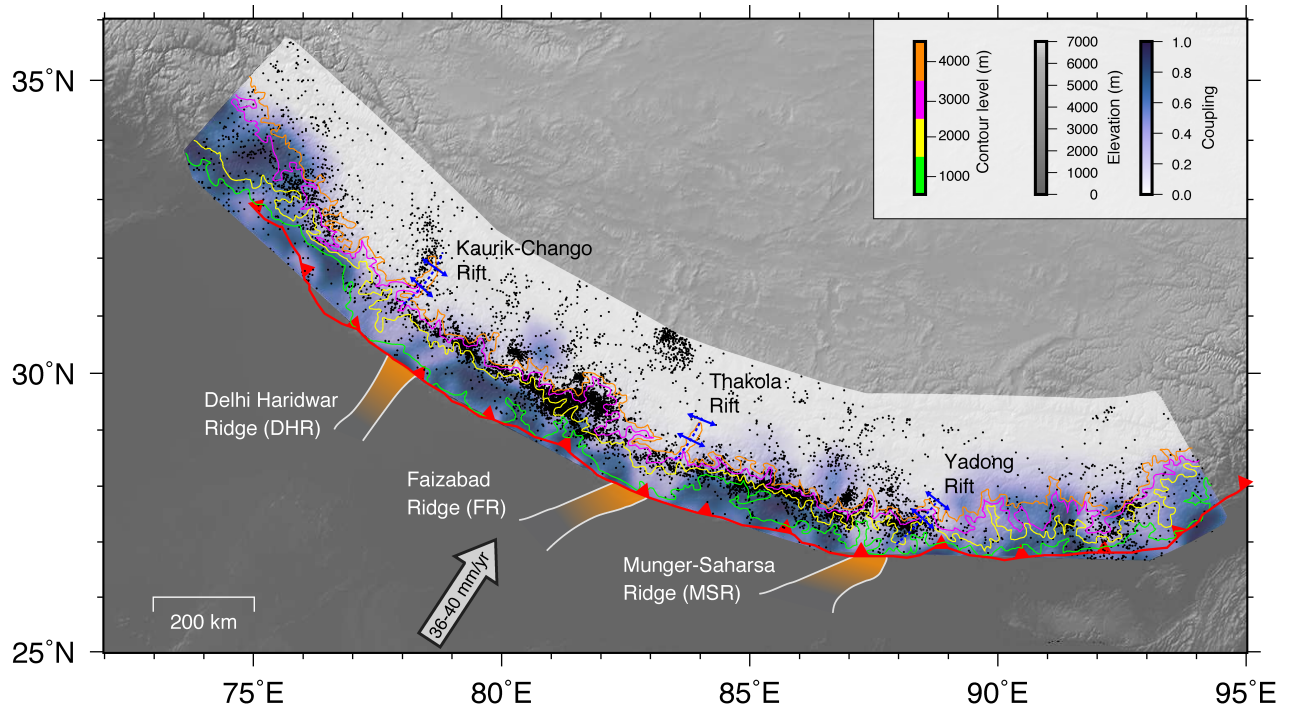


Figure S7. Comparison between topography, interseismic coupling, and (micro-)seismicity. Seismicity within Nepal is from an NSC catalog (Ader et al., 2012). Seismicity between $\sim 77^\circ\text{E}$ and 81°E is from Mahesh et al. (2013), and the remainder is from National Earthquake Information Center (NEIC). Solid coloured lines show the topography contour lines. Dashed blue lines indicate the location of the Kaurik-Chango, Thakola, and Yadong rifts. Orange patches indicate the location of the subsurface ridges beneath the Indo-Gangetic Plains. The Main Frontal Thrust is outlined in red.

References

- Ader, T., Avouac, J.-P., Liu-Zeng, J., Lyon-Caen, H., Bollinger, L., Galetzka, J., ... others (2012). Convergence rate across the nepal himalaya and interseismic coupling on the main himalayan thrust: Implications for seismic hazard. *Journal of Geophysical Research: Solid Earth (1978–2012)*, 117(B4).
- Ambraseys, N., & Douglas, J. (2004). Magnitude calibration of north indian earthquakes. *Geophysical Journal International*, 159(1), 165–206.
- Ambraseys, N., & Jackson, D. (2003). A note on early earthquakes in northern india and southern tibet. *Current Science*, 570–582.
- Avouac, J.-P., Ayoub, F., Leprince, S., Konca, O., & Helmberger, D. V. (2006). The 2005, mw 7.6 kashmir earthquake: Sub-pixel correlation of aster images and seismic waveforms analysis. *Earth and Planetary Science Letters*, 249(3-4), 514–528.
- Avouac, J.-P., Meng, L., Wei, S., Wang, T., & Ampuero, J.-P. (2015). Lower edge of locked main himalayan thrust unzipped by the 2015 gorkha earthquake. *Nature Geoscience*.
- Bendick, R., Bilham, R., Khan, M. A., & Khan, S. F. (2007). Slip on an active wedge thrust from geodetic observations of the 8 october 2005 kashmir earthquake. *Geology*, 35(3), 267–270.
- Berthet, T., Ritz, J.-F., Ferry, M., Pelgay, P., Cattin, R., Drukpa, D., ... Hetényi, G. (2014). Active tectonics of the eastern himalaya: New constraints from the first tectonic geomorphology study in southern bhutan. *Geology*, 42(5), 427–430.
- Bilham, R. (2004). Earthquakes in india and the himalaya: tectonics, geodesy and history. *Annals of Geophysics*, 47(2-3).
- Bilham, R., & Ambraseys, N. (2005). Apparent himalayan slip deficit from the summation of

- seismic moments for himalayan earthquakes, 1500–2000. *Current Science*, 88(10), 1658–1663.
- Bollinger, L., Sapkota, S. N., Tapponnier, P., Klinger, Y., Rizza, M., Van Der Woerd, J., ... Bes de Berc, S. (2014). Estimating the return times of great himalayan earthquakes in eastern nepal: Evidence from the patu and bardibas strands of the main frontal thrust. *Journal of Geophysical Research: Solid Earth*, 119(9), 7123–7163.
- Bollinger, L., Tapponnier, P., Sapkota, S., & Klinger, Y. (2016). Slip deficit in central nepal: omen for a repeat of the 1344 ad earthquake? *Earth, Planets and Space*, 68(1), 12.
- Duputel, Z., Vergne, J., Rivera, L., Wittlinger, G., Farra, V., & Hetényi, G. (2016). The 2015 gorkha earthquake: A large event illuminating the main himalayan thrust fault. *Geophysical Research Letters*, 43(6), 2517–2525.
- Galetzka, J., Melgar, D., Genrich, J. F., Geng, J., Owen, S., Lindsey, E. O., ... others (2015). Slip pulse and resonance of the kathmandu basin during the 2015 gorkha earthquake, nepal. *Science*, 349(6252), 1091–1095.
- Hetényi, G., Roux-Mallouf, L., Berthet, T., Cattin, R., Cauzzi, C., Phuntsho, K., ... others (2016). Joint approach combining damage and paleoseismology observations constrains the 1714 ad bhutan earthquake at magnitude 8 ± 0.5 . *Geophysical Research Letters*, 43(20).
- Hough, S. E., & Bilham, R. (2008). Site response of the ganges basin inferred from re-evaluated macroseismic observations from the 1897 shillong, 1905 kangra, and 1934 nepal earthquakes. *Journal of Earth System Science*, 117(2), 773–782.
- Khatti, K. (1987). Great earthquakes, seismicity gaps and potential for earthquake disaster along the himalaya plate boundary. *Tectonophysics*, 138(1), 79–92.

- Le Roux-Mallouf, R., Ferry, M., Ritz, J.-F., Berthet, T., Cattin, R., & Drukpa, D. (2016). First paleoseismic evidence for great surface-rupturing earthquakes in the bhutan himalayas. *Journal of Geophysical Research: Solid Earth*, *121*(10), 7271–7283.
- Lindsey, E. O., Natsuaki, R., Xu, X., Shimada, M., Hashimoto, M., Melgar, D., & Sandwell, D. T. (2015). Line-of-sight displacement from alos-2 interferometry: Mw 7.8 gorkha earthquake and mw 7.3 aftershock. *Geophysical Research Letters*, *42*(16), 6655–6661.
- Mahesh, P., Rai, S., Sivaram, K., Paul, A., Gupta, S., Sarma, R., & Gaur, V. (2013). One-dimensional reference velocity model and precise locations of earthquake hypocenters in the kumaon–garhwal himalaya. *Bulletin of the Seismological Society of America*, *103*(1), 328–339.
- Monsalve, G., Sheehan, A., Schulte-Pelkum, V., Rajaure, S., Pandey, M., & Wu, F. (2006). Seismicity and one-dimensional velocity structure of the himalayan collision zone: Earthquakes in the crust and upper mantle. *Journal of Geophysical Research: Solid Earth*, *111*(B10).
- Mugnier, J.-L., Huyghe, P., Leturmy, P., & Jouanne, F. (2004). Episodicity and rates of thrust-sheet motion in the himalayas (western nepal).
- Pandey, M., Tandukar, R., Avouac, J., Lave, J., & Massot, J. (1995). Interseismic strain accumulation on the himalayan crustal ramp (nepal). *Geophysical Research Letters*, *22*(7), 751–754.
- Pathier, E., Fielding, E., Wright, T., Walker, R., Parsons, B., & Hensley, S. (2006). Displacement field and slip distribution of the 2005 kashmir earthquake from sar imagery. *Geophysical Research Letters*, *33*(20).
- Sapkota, S., Bollinger, L., Klinger, Y., Tapponnier, P., Gaudemer, Y., & Tiwari, D. (2013).

- Primary surface ruptures of the great himalayan earthquakes in 1934 and 1255. *Nature Geoscience*, 6(1), 71–76.
- Sapkota, S. N., Bollinger, L., & Perrier, F. (2016). Fatality rates of the m w~ 8.2, 1934, bihar–nepal earthquake and comparison with the april 2015 gorkha earthquake. *Earth, Planets and Space*, 68(1), 40.
- Singer, J., Kissling, E., Diehl, T., & Hetényi, G. (2017). The underthrusting indian crust and its role in collision dynamics of the eastern himalaya in bhutan: Insights from receiver function imaging. *Journal of Geophysical Research: Solid Earth*, 122(2), 1152–1178.
- Thakur, V., Joshi, M., Sahoo, D., Suresh, N., Jayangondapermal, R., & Singh, A. (2014). Partitioning of convergence in northwest sub-himalaya: estimation of late quaternary uplift and convergence rates across the kangra reentrant, north india. *International Journal of Earth Sciences*, 103(4), 1037–1056.
- Wallace, K., Bilham, R., Blume, F., Gaur, V., & Gahalaut, V. (2005). Surface deformation in the region of the 1905 kangra mw= 7.8 earthquake in the period 1846–2001. *Geophysical Research Letters*, 32(15).